BILINGUAL PUBLISHING GROUP

Journal of Building Material Science
https://journals.bilpubgroup.com/index.php/jbms

ARTICLE

Load-Deformation Behaviour of Roof Truss System Made with Cold-Formed Steel Hollow Rectangular Section

Mohd Syahrul Hisyam Mohd Sani [1*], ***Cher Siang Tan*** [2], ***Fadhluhartini Muftah*** [1]

[1] *Faculty of Civil Engineering, Universiti Teknologi MARA (UiTM) Pahang Branch, Bandar Jengka 26400, Pahang, Malaysia*

[2] *Faculty of Civil Engineering, Universiti Teknologi Malaysia, Johor Bahru 81310, Johor, Malaysia*

ABSTRACT

The swift advancement of modern construction has established cold-formed steel (CFS) as a prominent structural option owing to its high strength-to-weight ratio and lightweight properties. However, CFS in open sections such as channel and zee sections is heavily restricted by susceptibility to premature instabilities such as local, distortional, and lateral-torsional buckling. The study examines the structural performance, especially the load-deformation behaviour of closed structural sections, to address and resolve these deficiencies and limitations. The main objective of the study is to experimentally determine the load-deformation behaviour of a full-scale roof truss system fabricated from a CFS hollow rectangular section and to compare it with that of a CFS channel section. A full-scale roof truss measuring 4,900 mm in span and 1,100 mm in height was constructed in a Howe configuration type and assembled using 6 mm self-drilling screws. Static vertical load experimental activity was conducted utilising a 100 kN load cell, a hydraulic jack, five linear variable deformation transducers (LVDTs), and seven strain gauges linked to a data logger to record ultimate load capacity, deformation and localised strain actions. The experimental results indicated that the CFS hollow outperforms the CFS channel section, attaining a 52.42% increase in ultimate load capacity and a 21.66% decrease in vertical mid-span deformation. The CFS channel had premature local and distortional buckling at its top chords, but the CFS hollow successfully mitigated early geometric instabilities. Ultimately, the study concludes that CFS hollow serves as a highly efficient, stiff and structurally stable system that is ideal for lightweight and sustainable long-span roofing applications.

*CORRESPONDING AUTHOR:
Mohd Syahrul Hisyam Mohd Sani, Faculty of Civil Engineering, Universiti Teknologi MARA (UiTM) Pahang Branch, Bandar Jengka 26400, Pahang, Malaysia; Email: msyahrul210@uitm.edu.my

ARTICLE INFO
Received: 1 June 2026 | Revised: 22 June 2026 | Accepted: 14 July 2026 | Published Online: 26 August 2026
DOI: https://doi.org/10.30564/jbms.v8i3.13582

CITATION
Mohd Sani, M.S.H., Tan, C.S., Muftah, F., 2026. Load-Deformation Behaviour of Roof Truss System Made with Cold-Formed Steel Hollow Rectangular Section. Journal of Building Material Science. 8(3): 159–174. DOI: https://doi.org/10.30564/jbms.v8i3.13582

Keywords: Load-Deformation Behaviour; Roof Truss System; Cold-Formed Steel; Hollow Rectangular Section; Channel Section

1. Introduction

The roof truss system is the main roof structure that is fabricated or constructed to shelter the building, house and factory from sunshine, rain, wind or snow, and must suit the architectural drawing. In general, the roof truss system is designed to sustain the self-weight of roofs and accessories, floors and internal loading such as ceilings, water storage, water conduits, and electrical and mechanical services. The roof truss system provides a stable and safe condition by supporting considerable loads for long span structures, is lightweight, and reduces deformation when subjected to internal and external loads. A roof truss system either in steel-based material, timber or matrix form is formed in a triangular shape that is able to transfer load in every section in compression and tension loads along them.

The roof truss system consists of the top and bottom chords, truss web members, and support and fastener, as shown in **Figure 1**. Normally, the roof truss system is one of the most important structural elements in a building and is available in a wide range of shapes, types, and configurations as shown in **Figure 2**. Various roof truss system configurations have been developed to meet certain structural specifications and service needs. The selection of a suitable roof truss system configuration is determined and governed by factors such as span length, roof pitch, loading conditions, construction cost, architectural functionality and material efficiency. Therefore, no single roof truss system configuration is suitable for all applications, and the selected system must offer the most effective load-transfer mechanism for the intended use and purpose. The roof truss system section for chord and truss web members is obtained in various shapes and sizes, such as open-section, such as channel, zee or angle sections, or hollow sections (closed-sections). They are also made by customising according to structural drawings and design, as well as architectural drawings. They are available in two-dimensional (2D) or three-dimensional (3D) trusses, which are built in various configurations and applications. A 2D truss is utilised for small and medium buildings and residential houses with low load capacity, and a 3D truss, also known as a space truss, is used for huge buildings such as airports, auditoriums, stadiums, and commercial buildings, which are normally exposed to high load capacity. There are a lot of studies of various types or configuration, such as flat truss [1–4] and space truss [5], but less research have focussed on other types of roof truss.

Nowadays, cold-formed steel (CFS) is recognised as a steel-based material that is replacing timber and hot-rolled steel as truss members, either chord or web members, due to its advantages, such as lightweight, fast production and installation, high strength-to-weight ratio, corrosion resistance, recyclability, and cost-effectiveness [6,7]. Bondok and Salim [8] have mentioned that CFS as a roof truss system material is categorised as a versatile structural material. CFS which is formed by cold-rolling and cold-pressing is more cost-effective in terms of performance when compared with hot-rolled steel which is formed at high temperature. CFS is formed in open-section and closed-section configurations that are proposed according to the application.

CFS trusses are commonly utilised in lightweight buildings, long-span structures, and modular construction, providing benefits such as diminished material consumption and expedited installation durations [6]. In contemporary civil engineering, CFS has become a leading material for light-to-medium-rise buildings and intricate roofing systems. Historically, CFS configurations have predominantly depended on open sections, including lipped and unlipped channel sections, or Zee sections. In the other study, there is a combination of using different sections in producing the CFS roof truss, such as the study by Gordziej-Zagórowska et al. [9], which combines a hat section and a channel section by using 6 M12 bolts, and Mahmoud et al. [3], which combines a hat section as the chord and a hollow section as a truss web member. The open-section is cheaper and easier to get from the construction material supplier than the closed-section. Although these sections provide exceptional customisability and fastening convenience, they are highly vulnerable to premature cross-sectional instabilities, including local, distortional, global and lateral-torsional buckling, which considerably restricts their compressive and torsional performance [10]. An example of premature cross-sectional instabilities is shown in **Figure 3**. Researchers have turned their attention to closed structural shapes by forming built-up sections utilising the fastener or using hollow sections such as rectangular hollow sections and square hollow sections to eliminate these geometric deficiencies. Wang et al. [11] mentioned that the built-up section in a box shape often displays axial strengths larger than the sum of their individual sections, and is suitable to be used as truss members for carrying axial load. Elsisi et al. [12] reported that the connection failure showed a significant impact on the performance of the full-scale CFS roof truss, which was made by combining the hat section as the chord, and the hollow section as the truss web member using screw in static and blast tests.

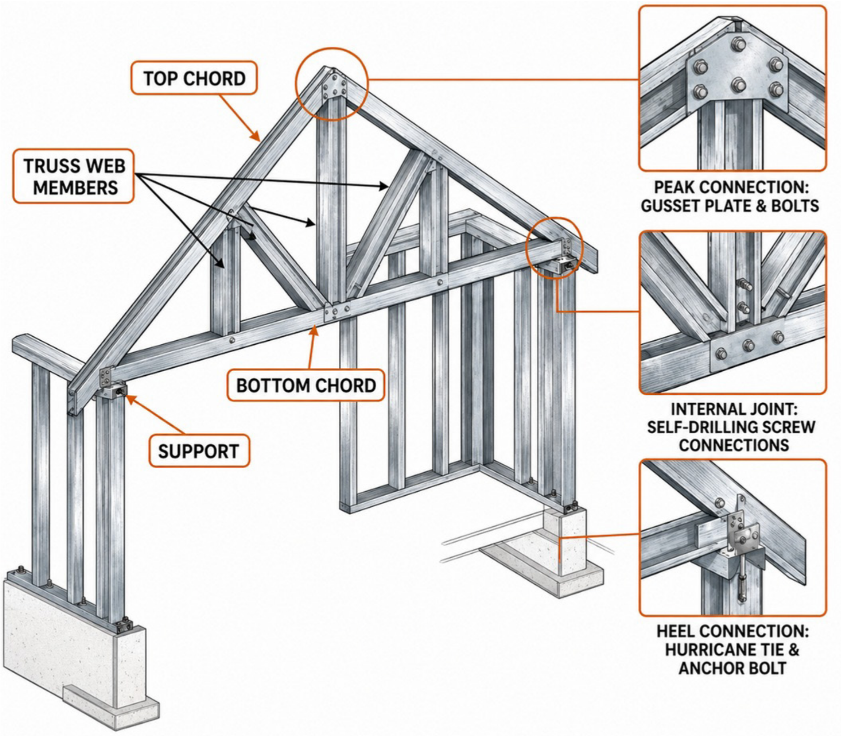

Figure 1. The roof truss system terminology.

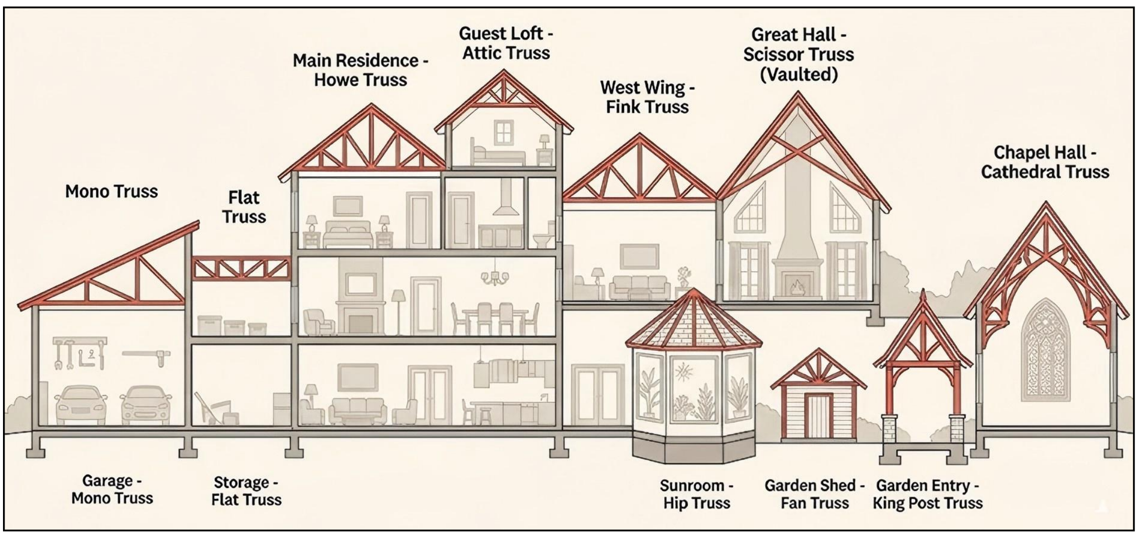

Figure 2. An example of the roof truss system configuration and application.

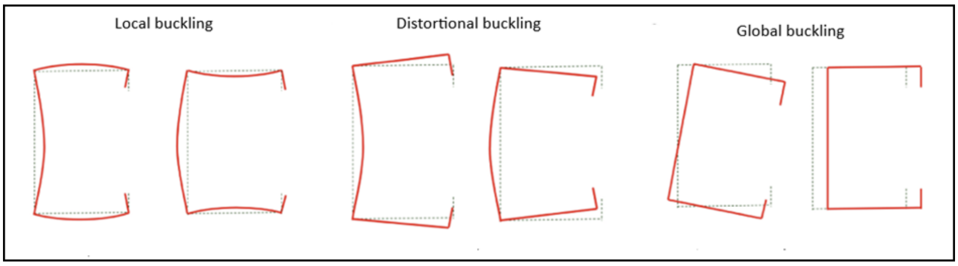

Figure 3. The example of the premature cross-sectional instabilities of the CFS channel [13].

The utilisation of hollow sections in CFS truss members confers significant structural benefits. The cold-forming manufacturing techniques modify the microstructural properties of the material, resulting in considerable strain hardening and increased strength, especially at the sharply bent corners of the hollow section [14]. In contrast to open sections, hollow geometries provide inherently enhanced torsional stiffness and well-proportioned radii of gyration across both major and minor axes [15]. When included in a long-span roof truss system design, these attributes significantly reduce unbraced lengths and enhance resistance to lateral-torsional buckling. Transitioning to hollow sections complicates joint details; traditional self-drilling screws may induce localised web crippling on tubular walls, necessitating the creation of advanced connections such as specialised gusset plates, high-strength bolted U-connectors, or nested sleeves to preserve structural integrity [16]. Li et al. [1] reported that the fasteners using screws and gusset plates of CFS truss members were often strengthened to provide the strength and stiffness requirements, and the experimental result showed that the gusset plates provided sufficient space for screw connections. Current academic emphasis integrates finite element analysis (FEA) with experimental validation to accurately delineate the interaction of material yield thresholds, initial geometric defects and localised buckling failure modes in close-section truss assemblies. Additionally, numerical studies employing FEA further support these findings, indicating that hollow sections exhibit stable deformation under gravitational and uplift loads. A recent study underscores the significance of comprehending buckling interaction, connection slip and stress redistribution in welded or screwed joints, as these factors substantially affect global load-deformation behaviour.

The ultimate load of a CFS roof truss is defined as the maximum external load that the truss system can withstand before failure occurs due to yielding, buckling, excessive deformation or connection failure. Unlike individual section design, the ultimate load of the overall roof truss is regulated by the interaction of section strength, global structural behaviour and connection performance. Both codes of practice, BS5950 (BS5950-5:1998) and Eurocode 3 (BS EN 1993-1-3), employ the limit state design philosophy, whereby the design resistance of every truss member and connection must be greater than the corresponding design action. The overall capacity of the roof truss is therefore determined by the weakest part or connection within the structural system. Analytical assessment of the ultimate load begins with a structural analysis, commonly performed using the matrix stiffness method or finite element analysis to calculate the axial load distribution in each truss member. The calculated member load is subsequently compared with their corresponding design resistance to establish the ultimate load-carrying capacity of the entire truss. According to BS5950, the ultimate resistances of the CFS roof truss are calculated using the following equations:

$$\text{Axial Tension Capacity, } P_t = A_e \times p_y \quad (1)$$

$$\text{Axial Compression Capacity, } P_c = A_{eff} \times p_c \quad (2)$$

Where:

A_e—Effective net area.

p_y—Design strength of the steel.

A_{eff}—Effective cross-sectional area determined by reducing the widths of slender elements using the effective width equation.

p_c—Compressive buckling strength, which depends on the slenderness ratio of the member.

According to Eurocode 3, the ultimate resistances of the CFS roof truss are calculated using the following equations:

Tension Resistance, $N_{t,Rd} = (A_{net} \times f_y)/\gamma_{M0}$ (3)

Compression Resistance, $N_{b,Rd} = (\chi \times \chi_d \times A_{eff} \times f_y)/\gamma_{M1}$ (4)

Where:

A_{net}—Net cross-sectional area.

f_y—Yield strength of the steel.

γ_{M0}—Partial factor for resistance of cross-sections.

A_{eff}—Effective area calculated using the element reduction factor, ρ for local buckling.

χ—Reduction factor for global flexural, torsional or flexural-torsional buckling.

χ_d—Reduction factor for distortional buckling.

γ_{M1}—Partial factor for resistance of members to buckling.

The previous studies have demonstrated that traditional CFS roof trusses constructed from open-sections, such as channel and Zee sections, are susceptible to local, distortional, global, and lateral-torsional buckling, frequently constraining their structural performance prior to the material attaining its maximum strength capacity. Whereas CFS hollow sections offer greater geometry efficiency, their implementation in roof truss systems is limited by a lack of sufficient experimental validation and published literature. This study provides novel insights by presenting experimental evidence regarding the influence of hollow section geometry on load-deformation behaviour, strain distribution, ultimate load capacity, structural stability, and failure modes within roof truss systems, thereby filling a critical gap in existing knowledge and offering essential guidance for the design and implementation of more efficient and stable lightweight steel roof structures. In conclusion, CFS hollow section roof trusses represent a viable structural system, providing strength, geometric efficiency and durability for contemporary lightweight roofing applications. As the industry increasingly emphasises sustainable and economically viable building methods, the high-strength-to-weight ratio of CFS provides a notable advantage by significantly diminishing the overall dead load of the roof structure, thereby reducing substructure, foundation and transportation costs. The study directly enhances structural safety and risk mitigation by thoroughly investigating ultimate load capacities, deflection limits, and failure modes. The study addresses a critical deficiency in light-gauge steel literature by establishing definitive, full-scale experimental baselines for load-deformation and load-strain under symmetric point loading, confirming that a hollow section doubles the ultimate load capacity and significantly stabilises high-stress compression zones. The main objective of the study is to determine the load-deformation behaviour of a roof truss system and the load-strain behaviour of truss members made with CFS hollow rectangular section, and compare it with a roof truss system made with CFS channel section.

2. Materials and Methods

The subtopic is described comprehensively in the experimental program section on material preparation and experimental setup. The material preparation includes the selection and characterisation of materials and dimensional specifications prior to experimental activity. Furthermore, the experimental setup is thoroughly explained, covering the equipment, loading arrangements, experimental procedure and data acquisition employed during the investigation.

2.1. Material Preparation

The load-deformation behaviour of the roof truss system made of CFS hollow rectangular sections was prepared and fabricated in three units. The hollow rectangular section is selected with dimensions of 40 mm × 75 mm × 1.00 mm, and the material strength is 550 N/mm^2 and other important information, such as material properties, is taken from the factory. The section properties of a hollow rectangular section are 174,363 mm^4 of I_x, 66,195 mm^4 of I_y, 27.78 mm of r_x, 17.11 mm of r_y, 4,604 mm^2 of Z_T, 4,348 mm^2 of Z_C, 122.92 mm^2 of A_{eff} and 205 kN/mm^2 of E. The span of the roof truss system is approximately 4,900 mm, and the configuration type for the roof truss system is the Howe configuration. The height of the roof truss system is 1,100 mm, and the clear span of 3,700 mm support to support. The roof truss member was joined using three or four self-drilling screws of 6 mm in diameter for each truss joint. Lastly, the channel section, which is used to compare with a hollow rectangular section in the roof truss system, has dimensions of 75 mm × 35 mm × 1 mm and a material strength of 550 N/mm^2.

2.2. Experimental Setup

The schematic diagram for the CFS hollow rectangular section roof truss system is illustrated in **Figure 4**, and the idea and arrangement of the experimental activity concerning the roof truss system pertain to the study conducted by Tam et al. [17]. The clear and real image of the experimental activity is shown in **Figure 5**. The substantial steel frame, steel spreader beam, steel plate hanger, solid wooden triangular blocks stopper, steel threaded rod, steel bracing, and bolts and washers were employed in the experimental setup. The end support condition is classified as a simple support. Six concentrated point loads were applied along the top chord with a spacing of 462.5 mm, commencing at the end support for each load. The weight was positioned on a strong and solid wood stopper with a steel plate hanger and connected by a double steel rod through the spreader beam. The spreader beam was positioned on the lower section of the roof truss system and the frame beam. The steel rods were connected to the spreader beam and secured using a washer and bolt. Additionally, five linear variable deformation transducers (LVDTs), seven strain gauges, a 100 kN load cell, a hydraulic jack, level measurement instruments and a data logger were included in the experimental setup.

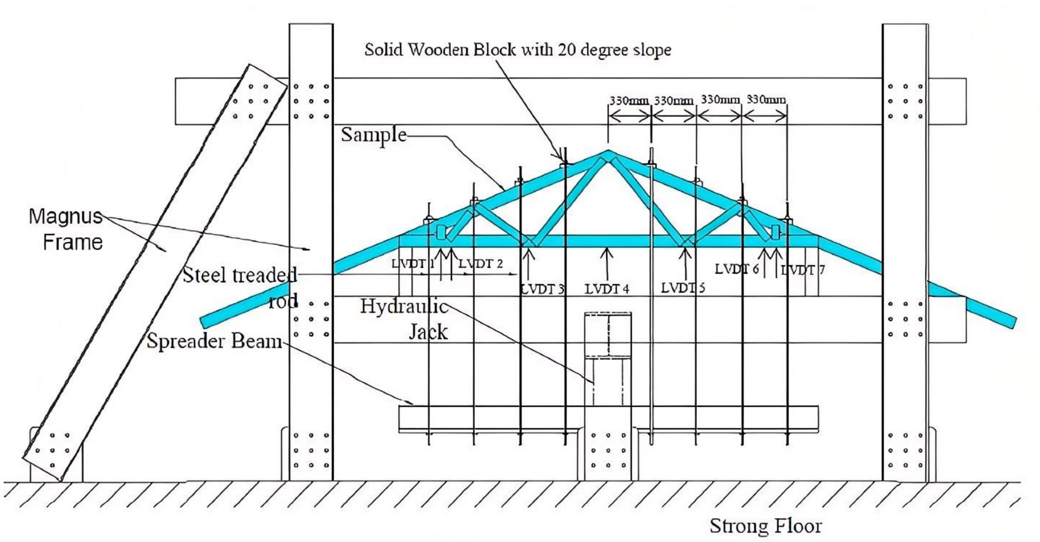

Figure 4. The schematic diagram of the idea and arrangement of the experimental activity [17].

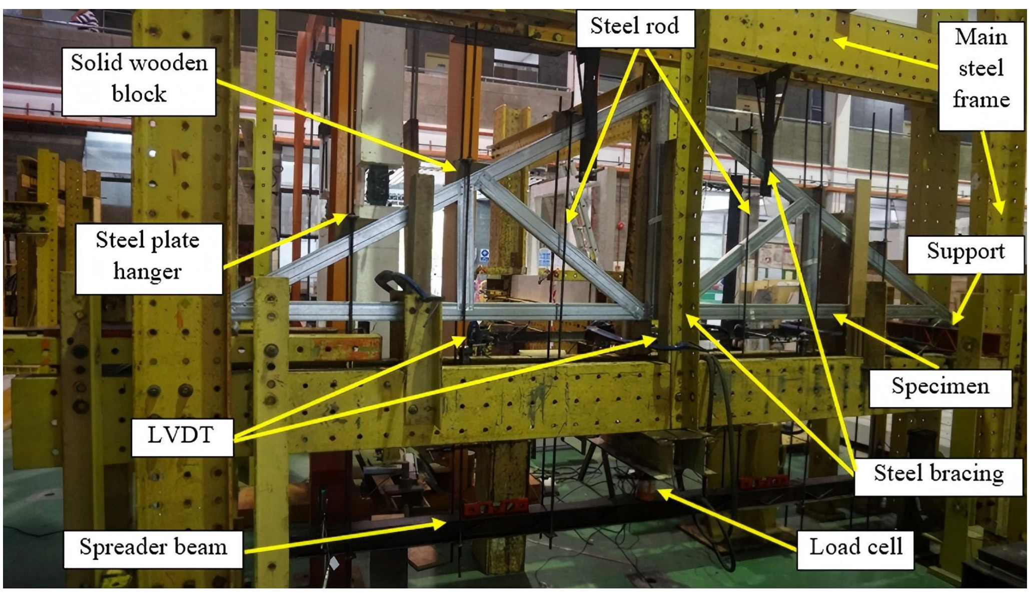

Figure 5. The experimental activity of the roof truss system arrangement in a real situation.

The load is exerted by pressing down on the spreader beam of identical dimensions and material with a hydraulic jack. When the spreader beam was pushed down, the double steel rod was similarly displaced downward, functioning as a concentrated load and combining to form a uniformly distributed load. Three level measurement instruments were positioned on the spreader beam at the left, centre and right to regulate the movement of the spreader beam in a consistently dispersed manner or uniformly distributed. The level measurement instruments were monitored every minute during the experiment to ensure the applied load remained consistent. Lastly, two LVDTs were positioned at the bottom of the spreader beam, one on the left side and one on the right side, to verify the movement of the spreader beam. As a conclusion, if the movement of the spreader beam descends consistently, the applied load utilised in the investigation is categorised as bearing the same load.

The load-deformation behaviour of the CFS hollow rectangular section roof truss system was tested, and all the necessary specimens and apparatus were prepared. The roof truss system was affixed to the main steel frame, which was anchored to a strong floor, with steel supports employed on both sides of the roof truss system. A steel plate featuring two holes was placed and connected to solid wooden triangular blocks by two self-drilling screws. The steel plate serves as a hanger for positioning the steel rod between the left and right sides of the roof truss system. The solid wooden triangular blocks were fixed on the top chord of the roof truss by using a self-drilling screw. Once the roof truss was secured to the steel frame, two steel rods were positioned on the steel plates on the left and right sides, accompanied by six solid wooden triangular blocks with steel plates. Each steel plate was affixed with two steel rods of varying lengths, contingent upon the location of the solid wooden block.

Upon the installation of the steel rod, the nuts on both the top and bottom sides of the steel rod were tightened and secured to the steel plate. The spreader beam that reacts as the load is distributed along the truss was located at the bottom side of the main steel frame beam and roof truss system. The second steel plate was positioned on the bottom side of the spreader beam and connected to a steel rod extending from the upper side of the steel plate. The steel rod was fixed in a straight orientation to guarantee the applied load from the vertical support from the top to the bottom sides. Thereafter, the nut was tightened on both the top and bottom sides of the second steel plate. The spreader beam was horizontally levelled, and its position could be modified by raising or lowering the steel plate and nuts.

After all nuts on the steel plate and roof truss were fixed, the load cells and hydraulic jack were positioned in the middle of the roof truss and came into contact with the surface of the spreader beam. Five LVDTs were situated on the roof truss; three LVDTs on the joint, and two LVDTs on the mid-span between the support and joint at the bottom chord, which is normally used to determine the deformation at the weakest part based on the study by Mohd Sani et al. [18] as shown in **Figure 6**. Subsequently, the seven strain gauges were affixed to seven truss members corresponding to their respective locations. Strain gauges were placed on horizontal (ST1 and ST2), vertical (ST3 and ST5) and inclined (ST4, ST6 and ST7) truss members to ensure that the strain of the truss member was either extension or contraction. All LVDTs, strain gauges and load cells were connected to a data logger via cables and wires. The experimental activity was started by applying the load using a manual hydraulic pump and jack, incrementally increasing the load by 1 kN. The applied load and experiment were stopped when the load reading diminished, and significant failure occurred. The data obtained from the LVDTs, strain gauge and load cells were compiled, and the failure mode of the roof truss was analysed and identified. The data collection determines the load-deformation behaviour, the load-deformation of the overall roof truss, and the strains of the roof truss members. The data of the experimental activity of the CFS hollow rectangular section roof truss system was compared with the data of the experimental activity of the CFS channel section roof truss system and with the design code of BS 5950 [19] and Eurocode 3 [20].

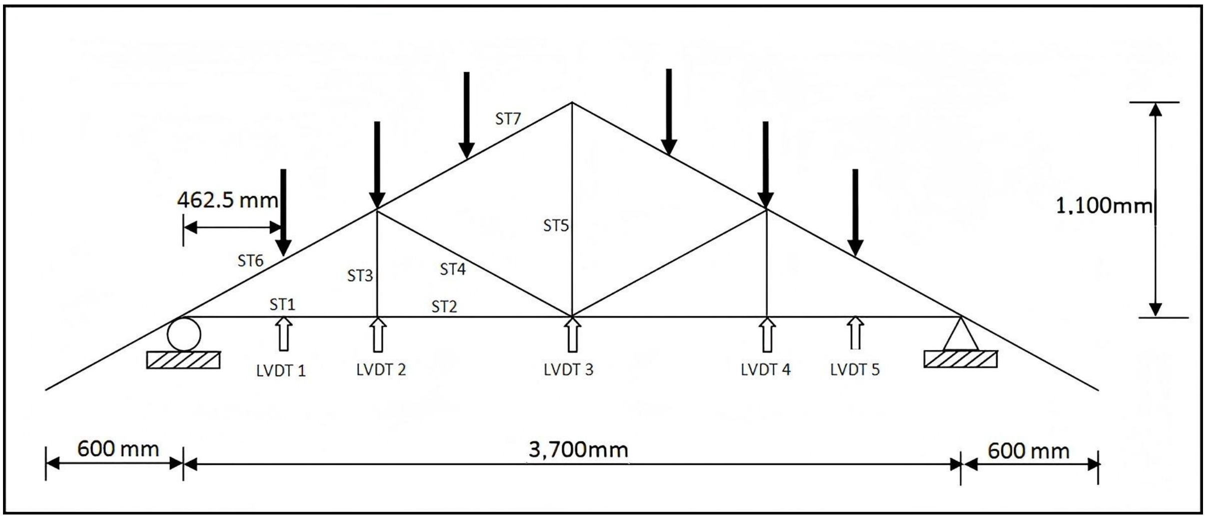

Figure 6. The schematic diagram of the location of loads, LVDTs and strain gauges.

3. Results and Discussion

The CFS hollow rectangular section and CFS channel section roof truss system was tested to determine the load-deformation behaviour and load-strain behaviour. The failure mode of the roof truss was observed, and lastly, the experimental data were compared with BS5950 [19] and Eurocode 3 [20].

3.1. Load-Deformation Behaviour of Overall Roof Truss

The results of the CFS hollow rectangular section (CFS hollow) and channel section (CFS channel) roof truss system with a span of 4,900 mm were tabulated in **Table 1**. The important parameters for determining the stability of the roof truss were its ultimate load and the deformation of the mid-span of the roof truss system. The highest value of ultimate load among the roof truss specimens is the CFS hollow. From **Table 1**, the percentage difference of ultimate load between the CFS hollow and CFS channel is approximately 52.42%, and the CFS hollow exhibited an ultimate load capacity approximately 110.15% larger than that of the CFS channel. Moreover, the percentage difference for deformation at mid-span of the roof truss system between CFS hollow and CFS channel is about 21.66%. The CFS channel had larger deformation at mid-span when compared with the CFS hollow. The ultimate load of the experiment was compared to the BS5950 and noted to have a ratio of 0.68 for CFS hollow and 0.36 for CFS channel. Furthermore, the ultimate load of the experiment was compared to Eurocode 3, which stated to have 0.81 for CFS hollow and noted having 0.77 for CFS channel. The Eurocode 3 ultimate load is more appropriate and relevant to compare with rather than BS5950. The load-deformation graph as shown in **Figure 7** clearly illustrates the structural superiority of the CFS hollow compared to the CFS channel. The CFS hollow exhibits a significantly steeper initial linear slope, representing substantially higher elastic stiffness and achieves more than double the ultimate load capacity, peaking at approximately 41.4 kN at a vertical deformation of around 17.0 mm before experiencing sudden structural failure. On the other hand, the CFS channel demonstrates a much lower structural stiffness, yielding early on and reaching a significantly lower peak load capacity of approximately 19.7 kN. Additionally, the CFS channel exhibits a highly unstable, undulating plateau between 15.0 mm and 21.70 mm of deformation with a classic signature of progressive, localised web crippling or premature distortional buckling typical of open sections.

The failure mode of the CFS hollow is reported to have the local buckling of the bottom chord near the support as shown in **Figure 8**, and the failure mode of the CFS channel is observed to have the local and distortional buckling of the top chord near the support as shown in **Figure 9**. The slender section in the CFS channel that is normally located at the bottom and top chords failed due to local buckling and then failed due to distortional buckling.

However, CFS hollow is able to minimise local and distortional buckling at the bottom and top chords. The design capacities predicted by BS 5950 and Eurocode 3 are excessively conservative, mainly because of their inability to precisely determine the precise failure position in the roof truss system made of CFS hollow sections.

Table 1. The result of the CFS hollow rectangular section and channel section roof truss system.

Specimen	Ultimate Load Experiment (kN)	Ultimate Load (kN)		Comparison		Deformation at Mid-Span	Failure Mode
		BS5950	Eurocode 3	P_{exp}/P_{BS5950}	$P_{exp}/P_{Eurocode\ 3}$		
CFS hollow	41.4	61.24	51.40	0.68	0.81	17.00 mm	Local buckling of the bottom chord near the support
CFS channel	19.7	55.40	25.70	0.36	0.77	21.70 mm	Local and distortional buckling of the top chord near the support

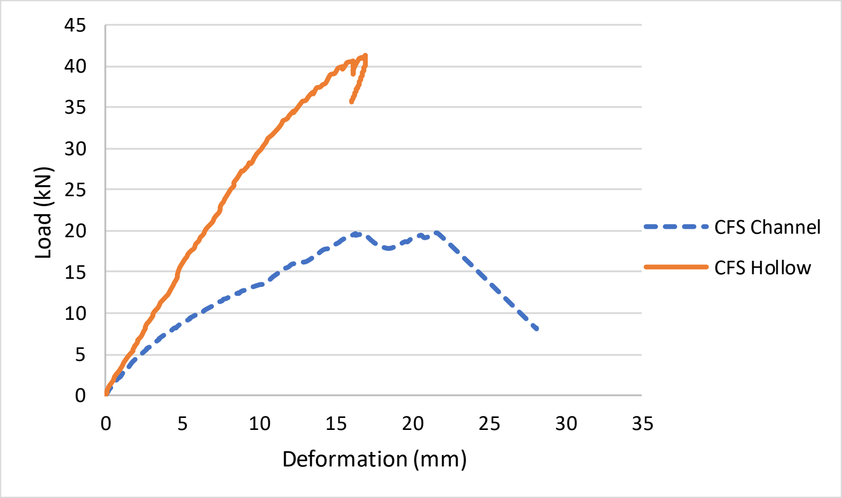

Figure 7. The load-deformation behaviour of CFS hollow and CFS channel.

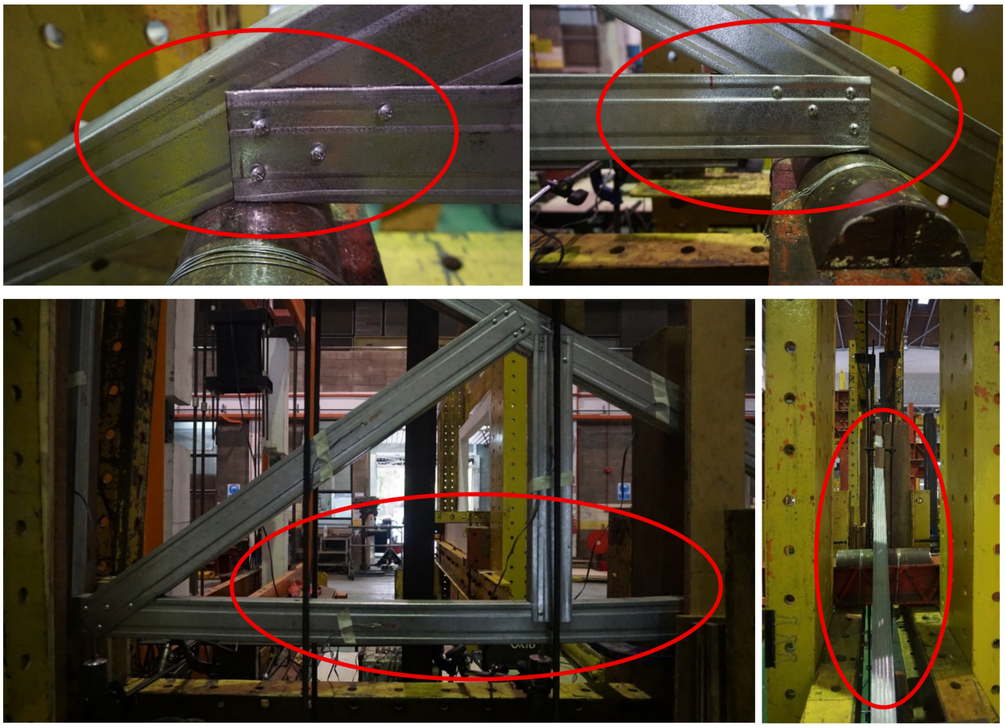

Figure 8. *Cont.*

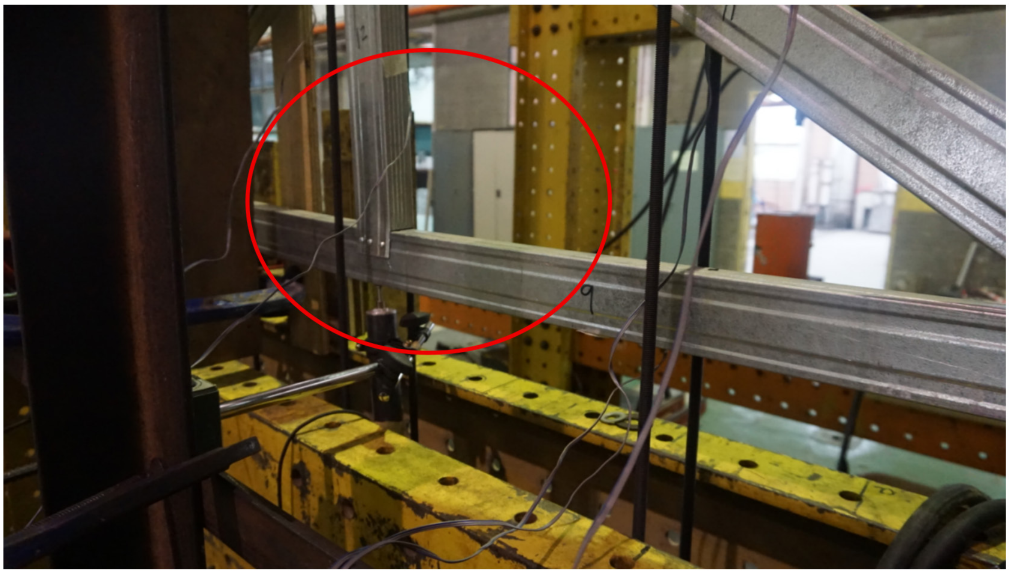

Figure 8. The buckling failure at the bottom chord of the CFS hollow.

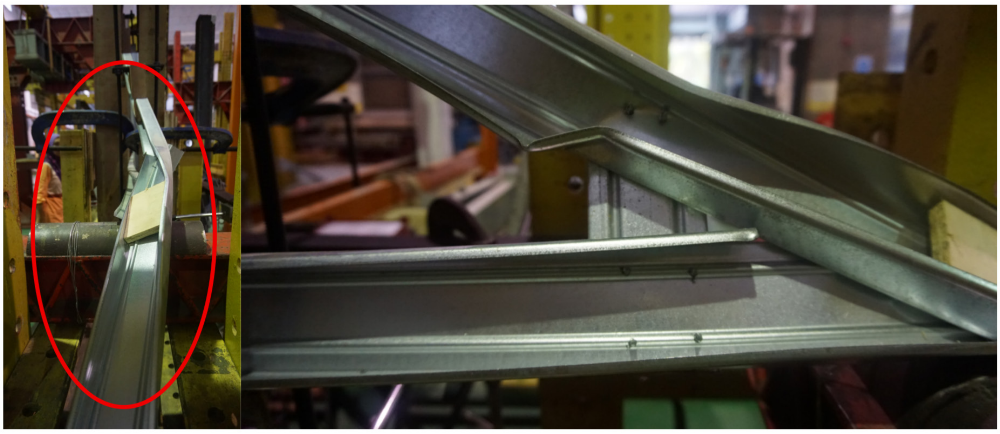

Figure 9. The buckling failure at the bottom and top chords of the CFS channel.

The other four locations of the LVDTs with the data on deformation at ultimate load for CFS hollow and CFS channel are tabulated in **Table 2**. The highest value of deformation at ultimate load for LVDT1, LVDT2, LVDT3 and LVDT4 is the CFS channel. The deformation at ultimate load at the joint of both specimens shows the highest value compared with the deformation at ultimate load at the mid-span between the support and joint at the bottom chord. The deformation at ultimate load of the CFS hollow at the left-hand side of the roof truss system is reported to have a lower value when compared with the right-hand side of the roof truss system. 19.17% and 8.75% are recorded for CFS hollow when the LVDT1 is compared with LVDT5, and LVDT2 is compared with LVDT4, respectively. Meanwhile, the deformation at ultimate load of the CFS channel on the right-hand side of the roof truss system is illustrated as more stable when compared with the left-hand side of the roof truss system. The difference in percentage between LVDT1 and LVDT5 for the CFS channel is 8.70%, and between LVDT2 and LVDT4 for the CFS channel is 8.29%. Furthermore, the percentage difference between the CFS hollow and CFS channel for LVDT1 is 39.75%, and for LVDT2 is 28.78%. However, the CFS channel is improved by around 14.89% for LVDT4 and 18.37% for LVDT5 when changed to CFS hollow. **Figure 10** illustrates the load-deformation behaviour of the CFS hollow for LVDT1, LVDT2, LVDT4 and LVDT5.

Table 2. The deformation at ultimate load for other locations of the CFS hollow and CFS channel.

Specimen	Ultimate Load (kN)	Deformation at Ultimate Load (mm)			
		Left-Hand Side		Right-Hand Side	
		LVDT1	LVDT2	LVDT4	LVDT5
CFS hollow	41.4	9.70	14.60	16.00	12.00
CFS channel	19.7	16.10	20.50	18.80	14.70

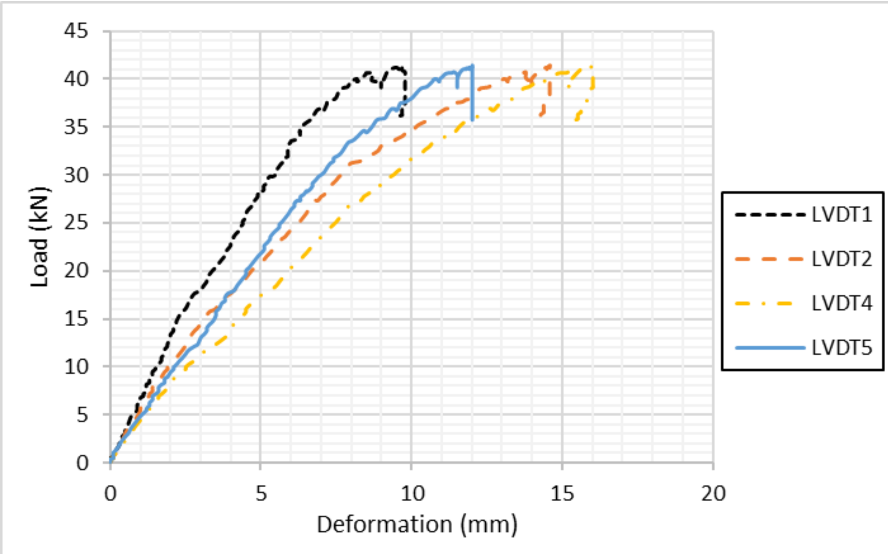

Figure 10. The load-deformation of the CFS hollow.

3.2. Load-Strain Behaviour of Truss Member

The result of the strain at the ultimate load of the truss member of CFS hollow and CFS channel is tabulated in **Table 3**. The experimental strain gauge data from the roof truss experimental activity reveal how structural profiles modify internal force pathways and cross-sectional stability under symmetrical downward loads. The highest values for horizontal location, vertical location and inclined location of the truss member for CFS hollow are ST2, ST3 and ST6, respectively. The strain distribution among the truss members aligns with classic truss mechanics, where the bottom chord observed by ST1 and ST2 registers positive strain values, indicating that the bottom chord effectively serves as a continuous tension strain to restrain the support system from spreading outward. Simultaneously, the vertical truss member at ST3 experiences a positive tension strain value due to the adjacent inclined or diagonal truss member exerting a downward and inward load at that particular panel zone under load, so placing the vertical post in a condition of tension. In contrast, the top chords at ST6 and ST7 exhibit significant negative strain values, affirming their function as a compression arch intended to direct the principal gravity loads downward to the supports, whereas the internal truss members at ST4 and ST5 display negative contraction values as they manage secondary compressive loads within the truss core. The critical part with high compressive strain is reported at the inclined truss member at the top chord.

Table 3. The result of the strain at the ultimate load of the CFS hollow and CFS channel.

Specimen	Ultimate Load (kN)	Strain at Ultimate Load (με)						
		ST1	ST2	ST3	ST4	ST5	ST6	ST7
CFS hollow	41.4	605	622	260	−242	−16	−1,008	−444
CFS channel	19.7	547	473	316	−473	−4	−1,316	−483

When comparing the cross-sectional efficiency of both roof truss systems, a significant behaviour difference is seen in the compression zones, underscoring the structural limits of the open section. The CFS channel exhibited a significantly higher compressive strain concentration at the critical top chord (ST6), attaining −1,316 με, in contrast to −1,008 με for the CFS hollow. This indicates that the CFS channel underwent more severe localised compressive deformation in the critical area despite its reduced load-bearing capacity. Additionally, the excessive strain contraction value in the CFS channel means that there is localised geometric distortion. This happens when the sides of the CFS channel that are not stiffened and standalone start to wrinkle, wave or buckle before they should. The Direct Strength Method, which was created by Yu and Schafer [21], has mentioned that open sections don't have torsional closure and are very likely to experience these localised cross-sectional instabilities long before the material hits its true yield limit. Ma et al. [14] confirmed that the CFS hollow has lower and more uniform strain concentrations across its compression elements because its closed tubular geometry provides continuous cross-sectional restraint, which delays distortional buckling and prevents early localised web crippling. The structural closure of the CFS hollow keeps its general shape and makes it more stable when it comes to bearing weight.

Specifically, the truss member of the CFS hollow is reported to have extension with tension load at the locations of ST1, ST2, and ST3, while the truss member with contraction value is stated at the locations of ST4, ST5, ST6 and ST7. Whilst the truss member of the CFS channel is similar to the CFS hollow, which recorded extension deformation at the locations of ST1, ST2 and ST3 and contraction deformation at the locations of ST4, ST5, ST6 and ST7. The percentage difference of the strain at ultimate load between CFS hollow and CFS channel is 9.59% for ST1, 23.95% for ST2, 17.72% for ST3, 48.84% for ST4, 75% for ST5, 23.40% for ST6 and 8.07% for ST7. **Figure 11** shows the load-strain behaviour of the CFS hollow, and **Figure 12** illustrates the location of the extension and contraction deformation on the overall roof truss system, either CFS hollow or CFS channel. In addition, the figure illustrates that the red colour is subjected to compression and the blue colour is subjected to extension, and the figure also effectively correlates the strain values with the truss shape and experimental observations. Comparable results have been documented in experimental and numerical investigations of CFS roof trusses, where increased truss member stiffness and improved connection stability led to greater load resistance and less localised deformation [22]. When the CFS channel section was compared with hat sections as chords in the roof truss system, Wang et al. [23] reported that the CFS hat sections demonstrated a more intricate failure behaviour, characterised by a combination of local and distortional buckling, spanning various truss members, in contrast to CFS channel sections, which were predominantly influenced by local buckling.

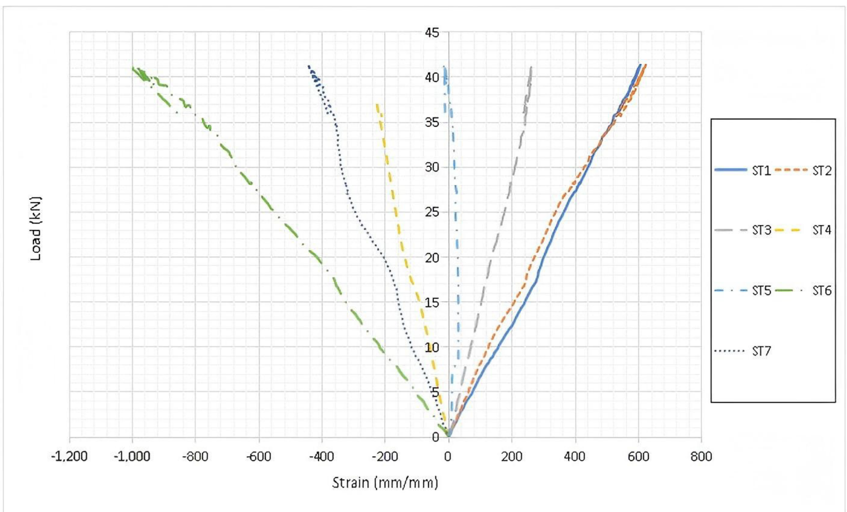

Figure 11. The load-strain behaviour of CFS hollow.

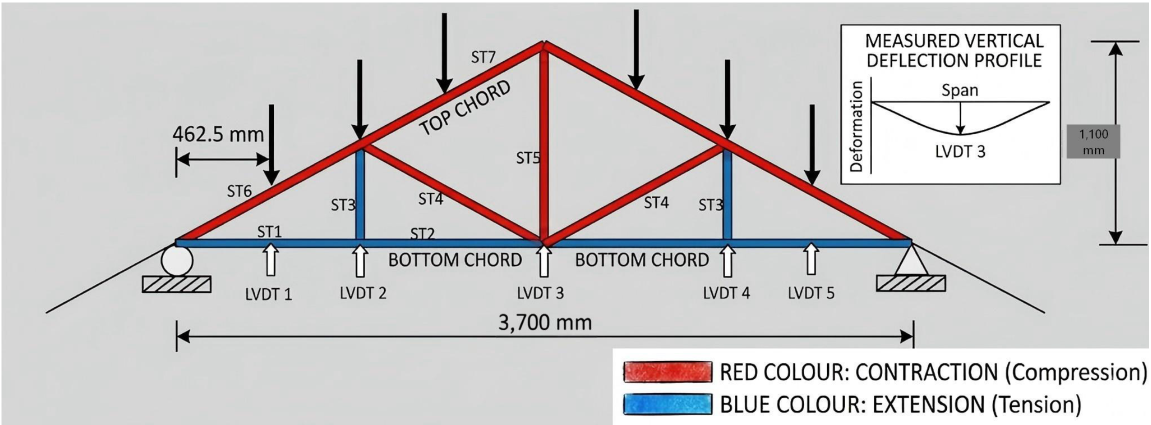

Figure 12. The location of extension and contraction deformation for the overall roof truss system.

In addition, the arrangement of truss members for the roof truss system also influenced the load-deformation behaviour of the overall roof truss and the load-strain behaviour of truss members. Normally, there are two types of structural truss member arrangement of the roof truss system: in-line truss and offset truss, as shown in **Figure 13**. In an in line truss, all truss web members and chords exist within a singular plane, and this is accomplished by coping the flanges of the channel sections to allow the webs to overlap and nest within one another. However, this coping process unfortunately results in localised web buckling. In a line truss, the features are normally similar to the arrangement of CFS hollow roof truss systems. Conversely, an offset truss comprises truss members and chords that do not exist in a single plane. Their truss web members are interconnected back-to-back, either by displacing the truss web members in relation to the chords or by displacing the bottom chord in relation to the top chord and webs. This offset arrangement enhances heel connection stability by minimising member rotation; nevertheless, the resultant loading eccentricity may induce warping and torsional stresses in the chords, hence reducing the overall load capacity of the truss. Dawe et al. [24] reported that the major failure is local buckling of the top chord at the heel plate for CFS offset trusses, while distortion or crippling of the heel plate beyond the ultimate load is only noted in specimens with unstiffened heel connections.

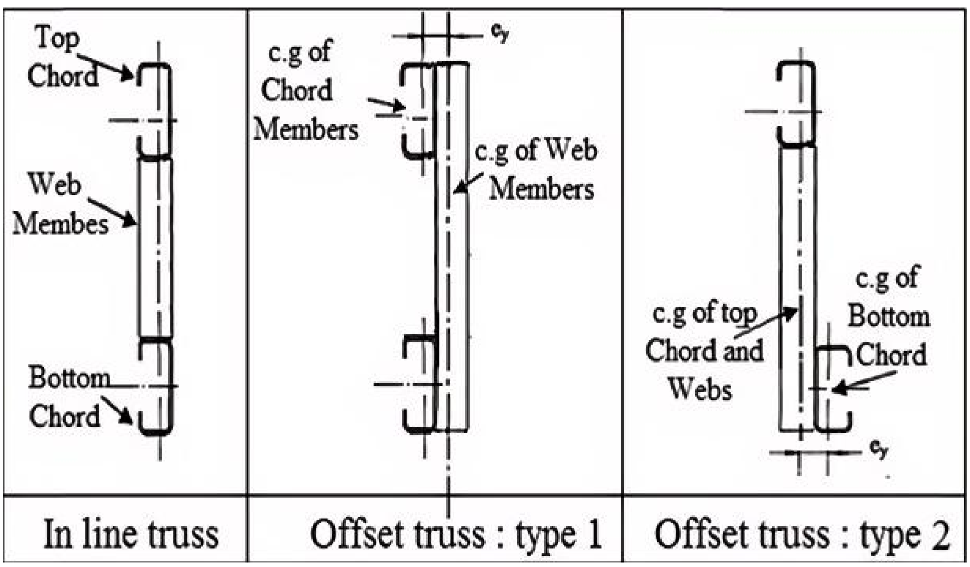

Figure 13. The arrangement of truss members using CFS channel [25].

4. Conclusions and Recommendations

The study is limited to the assessment of CFS hollow rectangular and CFS channel sections employed as a roof truss system subjected to static loading conditions. The comparison is limited to these two cross-sectional shapes, and the structural performance is assessed solely under static loads. Therefore, the findings may not be directly relevant to other CFS section geometries, roof truss system arrangements, and loading conditions. The experimental investigation successfully achieved the main objective of delineating the load-deformation of a CFS roof truss system and the load-strain behaviour of the truss web member made with a CFS hollow rectangular section. From the full-scale experimental activity, the CFS hollow produce a higher ultimate load when compared with the CFS channel. The experimental findings show that the CFS hollow surpasses the CFS channel, achieving a 52.52% enhancement in ultimate load capacity. A comparison analysis and observation demonstrate that the CFS hollow exhibits significantly greater load-bearing capacity and structural stiffness than the CFS channel. The ultimate load of the experiment for CFS hollow is found to have ratios of 0.68 when compared to BS 5950, and reported to have ratios of 0.81 when compared to Eurocode 3.

The CFS channel exhibited greater deformation at mid-span in comparison to the CFS hollow. Additionally, the CFS hollow reduced mid-span vertical deformations by approximately 21.66%, ensuring consistent elastic behaviour throughout its loading history. The failure mode of the CFS hollow is documented to exhibit local buckling of the bottom chord adjacent to the support. The enclosed cross-section of the CFS hollow enhances torsional rigidity, distributes stresses more uniformly and delays the onset of local buckling. As a result, the CFS hollow demonstrated better load-sharing capacity among its truss web members and attained a more balanced strain distribution.

The strain gauge measurements successfully verified the expected load distribution throughout the roof truss system. Tensile strains mostly occurred in the bottom chord, ST1 and ST2, and specific vertical truss web members, ST3, whereas compressive strains were concentrated in the inclined truss web members, ST4 that were far from the supports. The maximum compressive strain continuously occurred at ST6, identifying it as the most critical truss web member location. The results demonstrate that the CFS hollow displayed improved structural efficiency and stability relative to the CFS channel under the tested conditions, likely because of its superior stiffness and increased buckling resistance. The strain gauge measurements indicate that CFS hollow may exhibit higher load-carrying capacity compared to CFS channel under static loading conditions.

Based on the present findings of the study, the CFS closed-section exhibited favourable structural performance compared with the CFS open-section under the investigated static loading conditions. Although the findings suggest that closed-section CFS may offer advantages for medium-span and long-span light-gauge roof truss applications. Further experimental and numerical analysis encompassing a broader range of section geometries, loading conditions and connection details is required before such findings can be incorporated into engineering design guidelines. Future investigation and study should integrate finite element analysis to simulate the interactions of initial geometric imperfections, varying connection slip lengths and stress concentrations at the joint plates. Lastly, future research should systematically evaluate alternative high-strength bolted fasteners, gusset-plate reinforcements or nested sleeve orientations to safely enhance global load transfer mechanism efficiencies.

Author Contributions

Conceptualisation, M.S.H.M.S. and C.S.T.; methodology, M.S.H.M.S. and F.M.; validation, M.S.H.M.S. and C.S.T.; formal analysis, M.S.H.M.S. and F.M.; investigation, M.S.H.M.S. and F.M.; resources, C.S.T.; data curation, M.S.HMS. and F.M.; writing—original draft preparation, M.S.H.M.S. and F.M.; writing—review and editing, C.S.T.; project administration, M.S.H.M.S. and C.S.T.; funding acquisition, F.M. All authors have read and agreed to the published version of the manuscript.

Funding

The research was funded by the Ministry of Higher Education Malaysia via the Fundamental Research Grant

Scheme (FRGS/1/2023/TK06/UITM/02/11).

Institutional Review Board Statement

Not applicable.

Informed Consent Statement

Not applicable.

Data Availability Statement

The data used in the study are available from the corresponding author upon reasonable request.

Acknowledgments

The authors express their gratitude to the Ministry of Higher Education Malaysia for financing this research via the Fundamental Research Grant Scheme (FRGS/1/2023/TK06/UITM/02/11). We are equally obliged to the Faculty of Civil Engineering at Universiti Teknologi MARA (UiTM) Pahang Branch, whose superior experimental facilities and technical support constituted the foundation of our work.

Conflicts of Interest

The authors declare no conflict of interest.

AI Use Statement

The authors declare that no artificial intelligence (AI) tools were used in the preparation of this manuscript.

References

[1] Li, H., Shi, Y., Lu, W., et al., 2026. Flexural behavior of CFS trusses with strengthened joints. Thin-Walled Structures. 220, 114393. DOI: https://doi.org/10.1016/j.tws.2025.114393

[2] Li, H., Shi, Y., Peng, X., et al., 2025. Flexural behavior of parallel chord cold-formed steel trusses under serviceability limit states. Thin-Walled Structures. 215, 113568. DOI: https://doi.org/10.1016/j.tws.2025.113568

[3] Mahmoud, M.E., El-Sisi, A., Elbelbisi, A., et al., 2026. Effect of end-bearing connection configuration on static response of full-scale CFS trusses. Journal of Constructional Steel Research. 236, 109988. DOI: https://doi.org/10.1016/j.jcsr.2025.109988

[4] Mathieson, C., Clifton, G.C., Lim, J.B.P., 2016. Novel pin-jointed connection for cold-formed steel trusses. Journal of Constructional Steel Research. 116, 173–182. DOI: https://doi.org/10.1016/j.jcsr.2015.08.009

[5] Freitas, C.A.S., Yu, C., Nalla, S.K., 2026. Innovative continuous diagonal with stamped connections for cold-formed steel space trusses. Journal of Constructional Steel Research. 237, 110080. DOI: https://doi.org/10.1016/j.jcsr.2025.110080

[6] Freitas, C.A.S., Yu, C., Shahi, U., et al., 2025. Experimental and numerical study of a CFS truss with a stamped diagonal. Thin-Walled Structures. 217, 113870. DOI: https://doi.org/10.1016/j.tws.2025.113870

[7] Hussein, A.B., Papp, F., 2023. State-of-the-art: Integrating fastener technology and design guidelines for enhanced performance of cold-formed steel sections. Buildings. 13(9), 2338. DOI: https://doi.org/10.3390/buildings13092338

[8] Bondok, D.H., Salim, H.A., 2017. Failure capacities of cold-formed steel roof trusses end-connections. Thin-Walled Structures. 121, 57–66. DOI: https://doi.org/10.1016/j.tws.2017.09.026

[9] Gordziej-Zagórowska, M., Urbańska-Galewska, E., Deniziak, P., 2021. Analysis of failure mechanism in joints with positive eccentricity in CFS truss. Materials. 14(22), 6986. DOI: https://doi.org/10.3390/ma14226986

[10] Sam, V.S., Nammalvar, A., Andrushia, D., et al., 2024. Flexural behavior of galvanized iron based cold-formed steel back-to-back built-up beams at elevated temperatures. Buildings. 14(8), 2456. DOI: https://doi.org/10.3390/buildings14082456

[11] Wang, W., Roy, K., Rezaeian, H., et al., 2026. Structural behaviour of cold-formed steel trusses incorporating built-up section chords. Thin-Walled Structures. 218, 114054. DOI: https://doi.org/10.1016/j.tws.2025.114054

[12] Elsisi, A., Mahmoud, M.E., Salter, R., et al., 2026. Extreme static and blast performance of CFS roof trusses with symmetric profiles. Journal of Constructional Steel Research. 238, 110218. DOI: https://doi.org/10.1016/j.jcsr.2025.110218

[13] He, Z., Zhang, Y., Zhou, X., et al., 2024. Post-buckling behavior and DSM design of cold-formed steel lipped channel columns experiencing local-distortion-

al-global interaction. Structures. 67, 106945. DOI: https://doi.org/10.1016/j.istruc.2024.106945

[14] Ma, J.-L., Chan, T.-M., Young, B., 2017. Tests on high-strength steel hollow sections: A review. Proceedings of the Institution of Civil Engineers—Structures and Buildings. 170(9), 621–630. DOI: https://doi.org/10.1680/jstbu.16.00113

[15] Santaphan, S., Baskar, R., 2024. Experimental investigation on cold-formed steel structural frame made with lipped channel column and beam elements subjected to lateral loading. Revista Material. 29(3). DOI: https://doi.org/10.1590/1517-7076-rmat-2024-0323

[16] Lukačević, L., Krolo, P., Bakran, A., et al., 2023. Performance of novel U-connector in CFS truss-to-column bolted connection under axial force. Buildings. 13(7), 1623. DOI: https://doi.org/10.3390/buildings13071623

[17] Tam, P.H., Mohd Sani, M.S.H., Tan, C.S., et al., 2015. Force and Deformation Behaviour of Roof Truss System with Cold-formed Steel Channel Section. In Proceedings of the 9th Asia Pacific Structural Engineering and Construction Conference (APSEC) and 8th ASEAN Civil Engineering Conference (ACEC), Kuala Lumpur, Malaysia, 3–5 November 2015; pp. 180–189.

[18] Mohd Sani, M.S.H., Muftah, F., Tan, C.S., 2018. A state-of-the-art review on cold-formed steel roof truss system. International Journal of Civil Engineering and Technology. 9(9), 746–758.

[19] BS 5950-5:1998. 1998. Structural use of steelwork in building: Code of practice for design of cold-formed thin gauge sections.

[20] BS EN 1993-1-3:2006. 2006. Eurocode 3: Design of Steel Structures—Part 1–3: General Rules–Supplementary Rules for Cold-formed Members and Sheeting.

[21] Yu, C., Schafer, B.W., 2006. Distortional buckling tests on cold-formed steel beams. Journal of Structural Engineering. 132(4). DOI: https://doi.org/10.1061/(ASCE)0733-9445(2006)132:4(515)

[22] Bondok, D., Salim, H., Urgessa, G., 2021. Quasi-static responses and associated failure mechanisms of cold-formed steel roof trusses. Engineering Structures. 231, 111741. DOI: https://doi.org/10.1016/j.engstruct.2020.111741

[23] Wang, W., Roy, K., Rezaeian, H., et al., 2025. Moment capacity of cold-formed steel trusses with Howick Rivet Connectors: Tests, modelling and design. Engineering Structures 322, 119171. DOI: https://doi.org/10.1016/j.engstruct.2024.119171

[24] Dawe, J.L., Liu, Y., Li, J.Y. 2010. Strength and behaviour of cold-formed steel offset trusses. Journal of Constructional Steel Research. 66(4), 556–565.

[25] Reda, M., Sharaf, T., ElSabbagh, A., et al., 2019. Behavior and design for component and system of cold-formed steel roof trusses. Thin-Walled Structures. 135, 21–32. DOI: https://doi.org/10.1016/j.tws.2018.10.038